View Article Online / Journal Homepage / Table of Contents for this issue

PAPER

NJC
www.rsc.org/njc

Investigations of electron-transfer reactions and the redox mechanism of 2′-deoxyguanosine-5′-monophosphate using electrochemical techniques

Rajendra N. Goyal,* Sham M. Sondhi and Anand M. Lahoti

Department of Chemistry, Indian Institute of Technology Roorkee, Roorkee, 247 667, India. E-mail: rngcyfcy@iitr.erent.in

Received (in Montpellier, France) 5th October 2004, Accepted 23rd December 2004
First published as an Advance Article on the web 2nd March 2005

Downloaded by University of California - Los Angeles on 01 January 2013
Published on 02 March 2005 on http://pubs.rsc.org | doi:10.1039/B415452P

Electron-transfer reactions of 2′-deoxyguanosine-5′-monophosphate (dGMP) have been investigated in phosphate buffers of different pH at a pyrolytic graphite electrode (PGE). In cyclic voltammetry, two well-defined oxidation peaks, I_a (pH 1.9–10.6) and II_a (pH $\geq$ 5.8), were noticed. The peak potentials shifted towards less positive potential when pH was increased. Concentration and sweep rate studies established the adsorption of dGMP on the electrode surface. UV-vis spectral analysis at pH 2.9 and 7.1 indicated formation of a UV-absorbing intermediate, which decayed in a pseudo first-order reaction ($k = \sim 5.05 \times 10^{-4}$ s^{-1}). Coulometric, voltammetric and UV studies revealed the $4H^+$,$4e^-$ oxidation of dGMP by an EC (electrode reactions followed by chemical reactions) mechanism. The characterization of the oxidation products was achieved by converting them to their trimethylsilyl derivatives. At pH 7.1, 5-hydroxyhydantoin-5-carboxamide (**9**) and a N–O–C^8 linked trimer (**18**) and, at pH 2.9, monohydrated alloxan (**12**), deoxyriboside urea (**11**), two C^8O–OC^8 and one C^8–C^8 bridged dimers of dGMP (**13**, **14** and **15**, respectively) were formed as the major oxidation products. A tentative redox mechanism has been suggested for the electrooxidation of dGMP.

Introduction

Purine nucleotide 2′-deoxyguanosine-5′-monophosphate (dGMP) is one of the four essential deoxyribosyl nucleotides present in deoxyribonucleic acid (DNA) and is apparently a key compound in biological metabolism.[1] dGMP has been synthesized by oxidative phosphorylation of deoxyguanosine, catalyzed by deoxyguanosine kinase,[2–4] and is a precursor of the synthesis of 2′-deoxynucleoside diphosphate and triphosphate.[5,6] Apart from being a vital dietary nucleotide supplement,[7] dGMP has been widely used as a DNA model system in various biological studies. Studies of mutational changes in the DNA sequence caused by carcinogens present in cigarette smoke revealed that dGMP prevents double-stranded breaks, anaphase bridge formation and genomic imbalances.[8] Electron transfer from dGMP to the oxidized radical of riboflavin, studied using laser flash photolysis,[9–11] provided an imperative pathway to DNA damage both *in vivo* and *in vitro*. Fast electron repair of oxidizing OH adducts of dGMP by various acid derivatives, studied using pulse radiolysis,[12–14] is well-documented in the literature. Synthetic and spectroscopic studies of dGMP complexes with Pt(II), Mg(II)[15] and with other metal ions[16] have been topics of interest for chemists during the past decade.

Recent reports[17] from the American Health Foundation revealed that cyclic deoxyguanosine adducts formed by reaction of polyunsaturated fatty acids on dGMP under oxidative conditions are responsible for DNA lesions. Thus, electron-transfer reactions of dGMP are of significant importance for understanding the mechanism of oxidative damage in DNA.[18,19] Torun and Morrison[20] supported formation of singlet oxygen during photooxidation studies on dGMP. Still, a literature survey shows that very limited information is available on the electrooxidation[21] of dGMP. Although Compton *et al.*[22] have studied square-wave voltammograms of dGMP at a boron-doped diamond electrode, no attempt has been made to study the mechanism of the electron-transfer reactions and to identify the oxidation products of dGMP.

Electrochemical oxidation studies in combination with other instrumental methods, such as UV spectroscopy and mass spectrometry, provide invaluable information about biologically relevant redox reactions of important biomolecules.[23,24] Over the past few years, our laboratory has been actively involved in the investigation of redox properties of purine bases[25,26] and their nucleosides[27] and nucleotides,[28] using solid electrodes with the ultimate aim to elucidate the electron-transfer behavior of nucleic acids, DNA and RNA. In continuation of our efforts, it was considered worthwhile to study the electron-transfer reactions of dGMP (**1**) over a large pH range, using different electrochemical and analytical techniques.

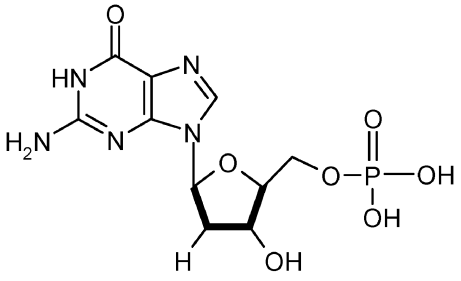

1

DOI: 10.1039/b415452p

This journal is © The Royal Society of Chemistry and the Centre National de la Recherche Scientifique 2005

View Article Online

Experimental

Materials and general procedures

The disodium salt of 2′-deoxyguanosine-5′-monophosphate (dGMP · Na_2) was purchased from Sigma (USA) and was used as received. Silylation grade acetonitrile and *N*,*O*-bis (trimethylsilyl)trifluoroacetamide (BSTFA) were from Pierce Chemical Co. (USA). Phosphate buffers of different pH and ionic strength were prepared[29] from analytical grade chemicals (NaH_2PO_4 and Na_2HPO_4 from Merck). The pH of the buffer solutions was measured using a Century India Ltd. digital pH-meter (model CP-901) after due standardization.

The voltammetric studies were carried out by using a pyrolytic graphite electrode (PGE; surface area: ~2.1 mm^2) from Pfizer and was fabricated by using a method reported in the literature.[30] The surface of the PGE was renewed after each voltammogram recording, by rubbing it with emery paper (C/P-400), cleaning the surface with water and gently drying it with tissue paper. As the electrode's surface area changed each time due to the cleaning process, the peak current values showed a variation of ±5%. Hence, voltammetric measurements were performed in triplicate and an average of the readings was taken as the final value. The working, counter and reference electrodes were pyrolytic graphite, platinum and Ag/AgCl electrodes, respectively. All potentials were referred to Ag/AgCl at ambient temperature, 25 ± 2 °C.

Cyclic sweep voltammetric studies were carried out by using a Cypress (model CS-1090) computer-controlled electroanalytical system. Coulometric experiments were performed by using a BAS CV-50W (model MF-9093) potentiostat. Controlled potential electrolysis (CPE) was carried out in a three-compartment cell using a pyrolytic graphite plate (6 × 1.5 cm^2) as working electrode, cylindrical platinum gauze (1.5 × 15 cm^2) as counter electrode and Ag/AgCl as reference electrode.

Spectral changes and kinetic studies associated with the electron-transfer reactions of UV-absorbing intermediates were monitored in a 1 cm quartz cell by using a Perkin–Elmer Lambda 35 UV-vis spectrophotometer. Gas chromatography/mass spectrometry analysis (GC-MS) of the silylated samples was performed with a Perkin–Elmer model Clarus-500 mass spectrometer. High performance liquid chromatography analysis was performed by using a Shimadzu modular HPLC. The IR spectrum of compound **9** was recorded in Nujol by using a Perkin–Elmer 1600 series FTIR spectrophotometer. The ^1H NMR spectrum of compound **9** was recorded in DMSO-d_6 with TMS as internal standard, by using a Brucker AC 300 F instrument.

A stock solution of dGMP (2.0 mM) was prepared using doubly distilled water. For voltammetric experiments 2.0 ml of the stock solution was mixed with 2.0 ml of phosphate buffer (1.0 M) of appropriate pH, so that the effective ionic strength of the solution would be 0.5 M. The solutions were deoxygenated by bubbling nitrogen gas for 8–10 min before recording the voltammograms. In the coulometric experiment a potential 100 mV more positive than the oxidation peak potential was applied to a 0.5 mM solution of dGMP. The number of electrons (*n*) involved in the oxidation reaction was determined by monitoring the exponential decay of the current *versus* time curve as reported by Lingane.[31] In spectral studies the progress of the electrolysis of a dGMP solution (0.1 mM) was monitored by withdrawing 2–3 ml of the sample from the working compartment of the H-cell at different time intervals and transferring them to a 1 cm quartz cell to record a UV spectrum in the 200–320 nm region. In another set of experiments, when absorbance at the λ_{max} was reduced to ~50%, the applied potential was turned off and the spectral changes of the solution were monitored at different time intervals. This helped to determine the wavelength region in which the UV-absorbing intermediates were generated during electrolysis. The decay of the absorbance with time was recorded at pre-selected wavelengths. The values of the rate constant (k) were calculated from the linear $\log(A-A_\infty)$ *versus* time plots.

For identification of the electrooxidation products, 10–15 mg of dGMP were bulk-electrolyzed in an H-cell. The three-electrode system used was essentially the same as that for the CPE experiment. The reference arm of the H-cell was filled with the buffer solution (pH 2.9 or 7.1), whereas the other arm was filled with a solution of dGMP at the same pH. Two arms of the H-cell were connected through a sintered disc filled with a KCl/Agar–Agar mixture. The electrolysis of the solution was carried out at a potential 100 mV more positive than that of peak I_a (see Fig. 1) for pH 2.9, or that of peak II_a for pH 7.1. Nitrogen gas was continuously bubbled through the solution under magnetic stirring during the course of electrolysis. The progress of electrolysis was monitored by recording cyclic voltammograms at different time intervals. When the oxidation peaks I_a or II_a disappeared, the exhaustively electrolyzed solution of dGMP was removed from the H-cell and sufficiently acidified (pH ~2) by adding a few drops of diluted HCl in order to convert the sodium salt into the corresponding free acid. The resulting solution was filtered and lyophilized. The freeze-dried material obtained was extracted with methanol (AR grade, 2 × 10 ml) and the methanolic extract was

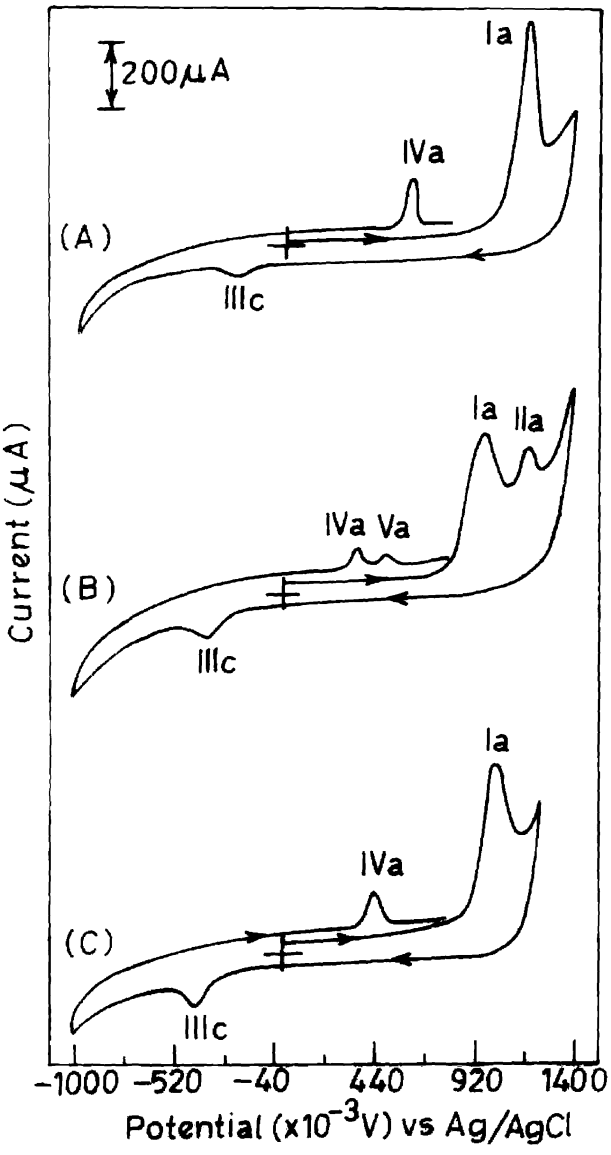

Fig. 1 Cyclic voltammograms of 1.0 mM dGMP at PGE: sweep rate 100 mV s^{-1} and phosphate buffers at pH 2.9 (A), 7.1 (B) and 7.1 with limited positive sweep potential (C).

Downloaded by University of California - Los Angeles on 01 January 2013
Published on 02 March 2005 on http://pubs.rsc.org | doi:10.1039/B415452P

View Article Online

concentrated and dried under reduced pressure. The product mixtures were converted to their thermally stable and volatile trimethylsilyl derivatives to allow GC-MS analysis.

Silylation was carried out in a 3.0 ml Reacti-vial (Pierce) glassware. *Ca.* 100 μg of the sample, acetonitrile (100 μl) and BSTFA (100 μl) were mixed in the vial, which was then carefully closed by using a Teflon-coated stopper and heated in an oil bath to 110 °C for 10–15 min with constant shaking. The vial was then allowed to cool down to room temperature and 5 μl of the sample was injected into the GC-MS apparatus; the spectrum was recorded in EI mode at 70 eV. HPLC was performed by using a reverse phase 250 × 4.6 mm 5μ Hypersin® BDS C_{18} column, an SPD-10A UV-vis detector, and an LC 10 AD pump with methanol–water (1.5 : 8.5) as the mobile phase.

Results and discussion

Voltammetry

A typical cyclic voltammogram of a 1.0 mM dGMP solution at pH 2.9 is depicted in Fig. 1(A). Below pH 5.8, at a sweep rate of 100 mV s^{-1}, dGMP exhibited a first well-defined oxidation peak I_a in the positive sweep. In the reverse sweep, an ill-defined cathodic peak III_c was noticed. In the next cycle, a new anodic peak IV_a was observed in the positive sweep, at a potential lower than I_a. To check whether peak III_c corresponds to the reduction of species generated by the oxidation occurring at peak I_a or is due to an independent reduction of dGMP, cyclic voltammograms were also recorded by initiating the sweep in the negative direction. It was observed that, in that case, no reduction peak III_c was obtained. Hence, it can be concluded that III_c is due to the reduction of a product resulting from the oxidation of dGMP at the potential of peak I_a.

At pH ≥ 5.8, the cyclic voltammogram of dGMP exhibited two anodic peaks, I_a and II_a, in the initial positive sweep. In the reverse sweep, reduction peak III_c was also noticed. In the following positive sweep, two ill-defined anodic peaks IV_a and V_a were recorded [see Fig. 1(B) for a typical example at pH 7.1]. Thus, peaks II_a and V_a are only observed at pH ≥ 5.8, whereas peaks I_a, III_c and IV_a are observed in the entire pH range. When the cyclic voltammogram was recorded at pH 7.1 in such a way that the direction of the sweep was reversed after the first oxidation (peak I_a) but before the second oxidation [peak II_a not recorded, Fig. 1(C)], peak V_a was no longer observed in the next cycle. This suggests that the species oxidized at the potential corresponding to peak V_a are related to those formed during the oxidation reactions occurring at the highest potential (peak II_a) in the first cycle. In other words, a relation between peak II_a and peak V_a is revealed.

In all cases, the potentials of the peaks were found to be dependent on pH and shifted to less positive values with increasing pH. Peak potential values (E_p) at different pH for peaks I–V are plotted in Fig. 2. The plots outline a linear relation between E_p and pH, which is transcribed in Table 1 for each peak.

The effect of concentration of dGMP, in the range 0.2–3.0 mM, on the peak current (i_p) of the well-defined peaks I_a and II_a was studied. The background current of the phosphate buffer was subtracted from the observed values of i_p. The plots of peak current *versus* concentration for peaks I_a and II_a are shown in Fig. 3. It is clear from these plots that i_p increases linearly with increasing concentration until ~2.0 mM, at which point the slope flattens noticeably. This behavior is generally indicative of adsorption complications[32,33] at the PGE electrode surface during reactions involving dGMP and was further confirmed by increasing the sweep rate v. This resulted in a linear increase of i_p, as well as an increase in the peak current function $i_p v^{-1/2}$ as log$v$ increased. Fig. 4 shows the

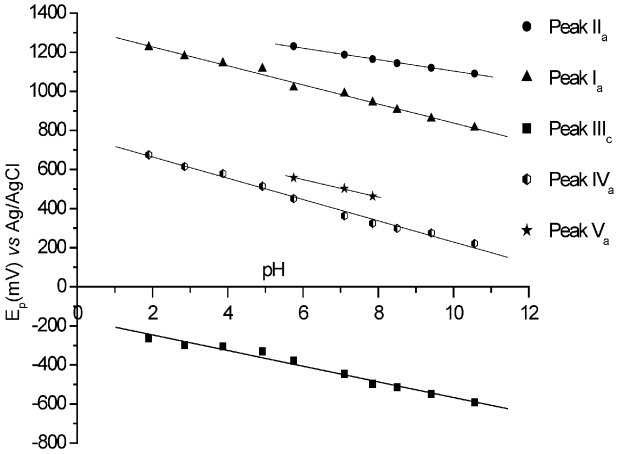

Fig. 2 Observed variations of peak potentials with pH for 1.0 mM dGMP at PGE with a sweep rate of 100 mV s^{-1}.

plot of $i_p v^{-1/2}$ *versus* log$v$, which can be represented by two nonlinear curves. Such a behavior suggests a change in mechanism at around log v = 1.7.

The effect of sweep rate on peak potentials was also studied at pH 7.1 in the sweep range 10–1000 mV s^{-1}. At sweep rates >700 mV s^{-1}, the peaks became very broad and merged with the background. The linearity of the plots of the potential of peaks I_a and II_a *versus* log$v$ changed at around log v = 2.3, as shown in Fig. 5. Thus, at sweep rates ~200 mV s^{-1}, the mechanism of electrooxidation of dGMP appeared to change from diffusion-controlled to a more complicated one due to adsorption.

In coulometric experiments, the number n of electrons involved in the electrooxidation of dGMP at different pH was calculated from the graphical integration of the current *versus* time curve.[31] The plots of peak current *versus* time were exponential for the first 15 min of electrolysis and thereafter deviation from a straight line was noticed. This deviation clearly indicates that during the first 15 min, the reactions at the electrode followed a simple pathway and, thereafter, subsequent chemical reactions played an important role. Similar observations have been reported by Cauquis and Parker[34] on charge-transfer reactions coupled with follow-up chemical reactions, that is, EC (electrode reactions followed by chemical reactions) mechanisms. The average experimental value of n at different pH was 3.9 ± 0.25.

Spectral study

UV spectra were recorded at different time intervals during the electrochemical oxidation of 0.1 mM dGMP at pH 2.9 in order to detect the formation of UV-absorbing intermediates (Fig. 6). The spectrum of dGMP before oxidation exhibits two well-defined absorption bands at 200 and 255 nm (λ_{max}) and a shoulder at 280 nm (curve a in Fig. 6). Upon application of a potential E_p of 1.31 V, that is, 100 mV more positive than $E_p(I_a)$, absorbance in the ranges 195–210 and 235–295 nm

Table 1 Peak potential E_p and pH relations calculated from Fig. 2 for peaks I–V (from CV of 1.0 mM dGMP)

	E_p and pH relation		
Peak	pH range	E_p (*vs.* Ag/AgCl)/mV	Correlation coefficient
I_a	1.9–10.6	1363.7 – 53.69 × pH	0.976
II_a	5.8–10.6	1395.3 – 29.2 × pH	0.997
III_c	1.9–10.6	−160.8 – 40.6 × pH	0.972
IV_a	1.9–10.6	770.9 – 53.6 × pH	0.974
V_a	5.8–07.9	816.4 – 44.7 × pH	0.995

Downloaded by University of California - Los Angeles on 01 January 2013
Published on 02 March 2005 on http://pubs.rsc.org | doi:10.1039/B415452P

View Article Online

Downloaded by University of California - Los Angeles on 01 January 2013
Published on 02 March 2005 on http://pubs.rsc.org | doi:10.1039/B415452P

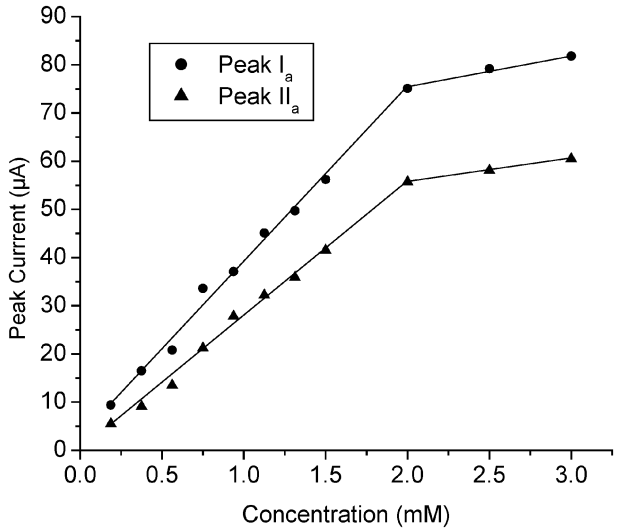

Fig. 3 Dependence of the current intensity (i_p) of peaks I_a and II_a on the concentration of 1.0 mM dGMP at pH 7.1.

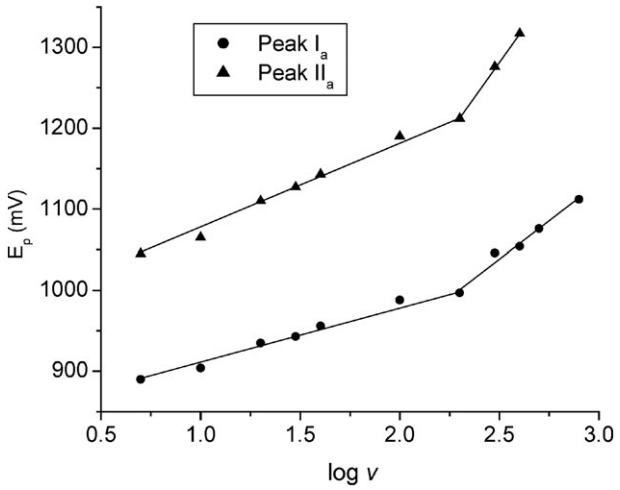

Fig. 5 Variation of peak potentials I_a and II_a with log$v$ for 1.0 mM dGMP at pH 7.1.

decreased, while absorbance in the ranges 210–235 and 295–320 nm increased. In curve i, which was recorded after 120 min of electrolysis, the band at 250 nm has almost completely disappeared (Fig. 6). Three isosbestic points are clearly noticed at 210, 238 and 295 nm.

At pH 7.1, a 0.1 mM solution of dGMP exhibited two well-defined absorption bands at λ_{max} = 205 and 255 nm and a shoulder at 275 nm. The spectral changes due to the electrochemical oxidation of dGMP at pH 7.1 were essentially the same as those observed at pH 2.9. However, upon application of a potential E_p = 1.29 V (100 mV more positive than that of peak II_a), absorbance in the ranges 210–200 nm and 240–295 nm decreased, while absorbance in the ranges 210–235 nm and 295–320 nm increased. After 120 min of electrolysis, it was found that the peak at 250 nm had completely disappeared and a new strong absorption band at 225 nm had appeared. No clear isosbestic point was observed in this case.

In another set of experiments, after electrolyzing the solution of dGMP for 45 min (when λ_{max} reaches ~50%), the potentiostat was open-circuited and UV spectra were recorded at different time intervals. It was observed that absorbance in the range 220–290 nm continued to decrease, due to the decay of the intermediate generated during the electrooxidation. Thus, a UV-absorbing electroactive intermediate is generated upon oxidation of dGMP and decays due to involvement in subsequent chemical reactions, which corresponds to an EC mechanism. The kinetics of decay of the UV-absorbing intermediate were monitored by recording the absorbance at selected wavelengths (230, 255 or 280 nm) as a function of time. The absorbance *versus* time profiles at different wavelengths showed an exponential decay (see for example Fig. 7, at 255 nm) and the plots of $\log(A - A_\infty)$ *versus* time (where A_∞ and A are the absorbance at infinite time and at the reaction time, respectively) were linear (see inset of Fig. 7). The pseudo-first-order rate constant values k for the decay of the UV-absorbing intermediate generated during the electrooxidation of dGMP at different pH were calculated from the slopes of the linear best fit equations corresponding to each $\log(A - A_\infty)$ *versus* time plot, and are listed in Table 2.

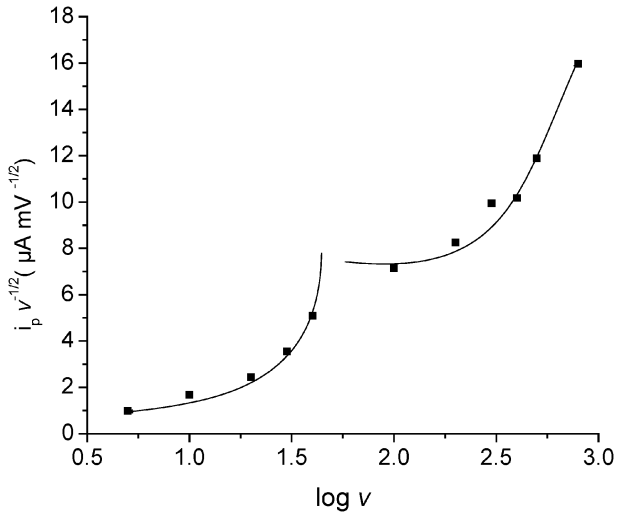

Fig. 4 Variation of the peak current function ($i_p v^{-1/2}$) for peak I_a with the logarithm of the sweep rate for 1.0 mM dGMP at pH 7.1.

Product characterization

Attempts to separate the different constituents and determine their molar masses from the exhaustively electrolyzed (at pH 2.9 and 7.1) samples of dGMP were unsuccessful, probably due to their nonvolatile nature. Hence, the electrooxidation products of dGMP were first converted to their thermally stable, volatile trimethylsilyl derivatives. This procedure has been found to be useful in characterizing the electrooxidation products of various biomolecules.[35]

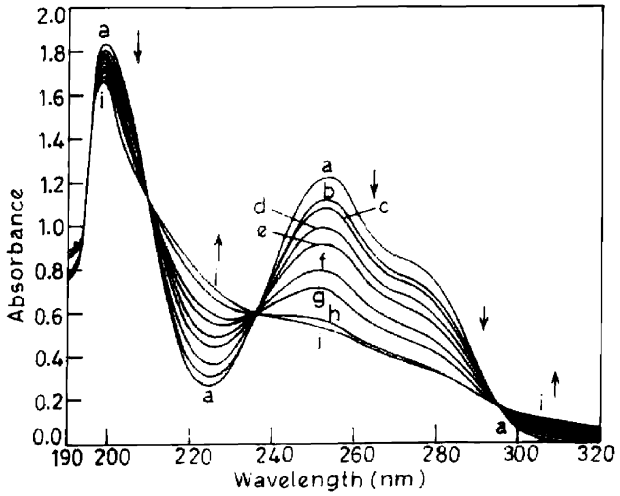

Fig. 6 Spectral changes with time during the electrochemical oxidation of 0.1 mM dGMP at pH 2.9 at E_p = 1.31 V [> $E_p(I_a)$ = 1.21 V]; spectra recorded after (a) 0, (b) 5, (c) 10, (d) 20, (e) 30, (f) 45, (g) 60, (h) 90, (i) 120 min of electrolysis.

View Article Online

Downloaded by University of California - Los Angeles on 01 January 2013
Published on 02 March 2005 on http://pubs.rsc.org | doi:10.1039/B415452P

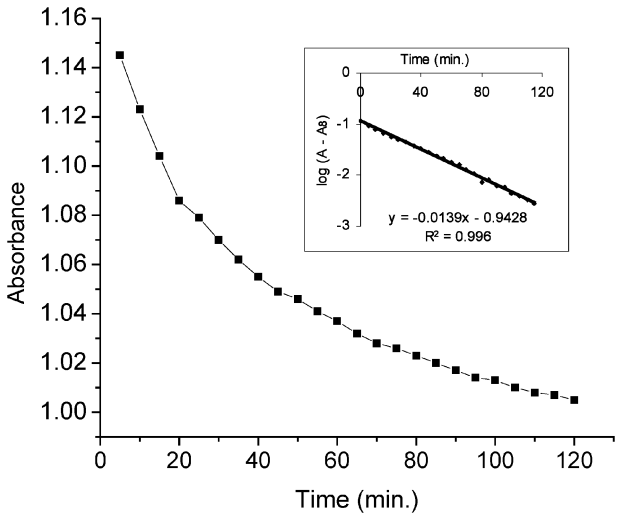

Fig. 7 Plots of absorbance at 255 nm *versus* time and $\log(A - A_\infty)$ *vs.* time (inset) for the decay of the UV-absorbing electroactive intermediate generated during the electrooxidation of 0.1 mM dGMP at pH 2.9.

The GC-MS analysis of the silylated sample at pH 7.1 was performed and two major peaks were detected at retention times R_t = 5.98 and 6.42 min (see corresponding MS spectra in Fig. 8). In acidic medium (pH 2.9), five major peaks were recorded at R_t = 4.35, 7.35, 7.42, 9.88 and 11.1 min. The corresponding molar masses and the relative abundances of the main peaks for each GC peak are presented in Table 3.

At pH 7.1, the products corresponding to R_t = 5.98 and 6.42 min were identified as being the tetrasilylated derivative of 5-hydroxyhydantoin-5-carboxamide [**9**, *m*/*z* 447 (M^+; 30.5%)] and the hexasilylated derivative of an N–O–C-linked trimer **18** [*m*/*z* 898 (M^+; 15.5%)], respectively (see Schemes 1–3). 5-Hydroxyhydantoin-5-carboxamide is one of the most well-known metabolites of purines and is reported[36,37] to undergo silylation at four sites. The trimer **18** (calcd 897.338 for $C_{34}H_{59}N_{13}O_5Si_6$) seems to be formed by three monomer units of dGMP, from which the deoxyribose sugar moiety of all three monomers has been lost during the reaction at the electrode surface. This observation is based on a comparison of the observed molar mass and mass calculations for different silylated trimer derivatives, with and without deoxyribose units. One of the possible reasons for losing the sugar units could be the strong steric hindrance implied by the trimerization. Formation of trimers during the electrooxidation of purine nucleosides has already been described in the literature[38] and obtaining a trimer as the oxidation product of dGMP at PGE is not unusual.

Scheme 1 describes the synthesis of the tetrasilylated derivative **9a** from **9** using BSTFA as the silylating agent and acetonitrile under anhydrous conditions. It is clear from Scheme 1 that compound **9** possesses five silylation sites and it can be expected that the reaction would take place at each of the available sites. However, the OH group situated between

Table 2 Pseudo-first-order rate constant values calculated for the decay of the UV-absorbing intermediate generated during the electrooxidation of dGMP.

pH	λ/nm	$k/10^{-4}$ s^{-1a}
7.1	280	4.85 ± 0.02
	255	5.02 ± 0.04
	230	4.84 ± 0.02
2.9	280	5.10 ± 0.04
	255	5.33 ± 0.02
	230	5.14 ± 0.02

[a] Average of at least three replicate determinations.

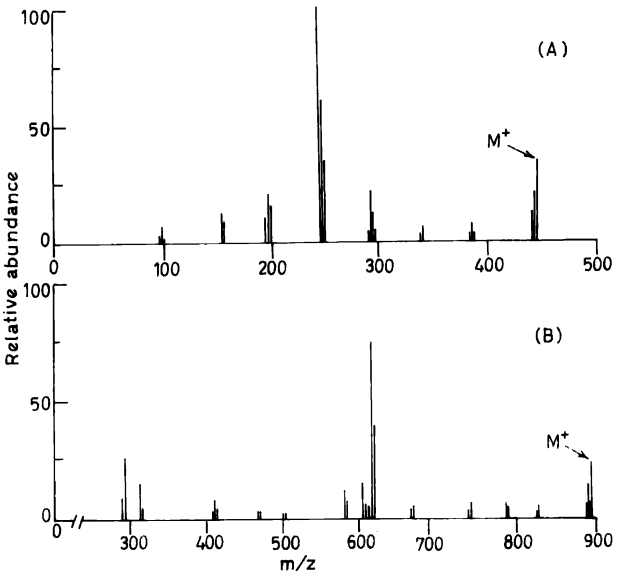

Fig. 8 Mass spectra recorded for peaks at R_t = 5.98 (A) and 6.42 (B) min from the GC-MS analysis of the silylated sample at pH 7.1 after electrooxidation above $E_p(II_a)$.

the C=O and NH functions does not permit silylation due to the bulky nature of the $Si(CH_3)_3$ group and compound **9a** was indeed identified by GC-MS at R_t 5.98 min with *m*/*z* 447 (calcd 447.186 for $C_{16}H_{37}N_3O_4Si_4$).

At pH 2.9, the peaks at R_t 4.35 and 11.1 min correspond to the molar masses 392 (M^+; 25.0%) and 448 (M^+; 20.5%), respectively. These molar masses are associated with the trisilylated derivative of urea deoxyriboside (**11**) and the tetrasilylated derivative of 5,5-dihydroxypyrimidine-2,4,6-trione (**12**), also know as hydrated alloxan (see Scheme 2).[26] Silylation of urea deoxyriboside has been considered to occur only on one side of the C=O group having the deoxyribose unit. A similar one-side silylated product of urea riboside has also been reported to form during the electrochemical oxidation of 9-β-D-ribofuransyluric acid.[39] The peaks at R_t 7.35 and 7.42 min correspond to the molar masses 952 (M^+; 16.9%) and 764 (M^+; 22.3%), respectively, and the corresponding products were identified as the hepta- and hexasilylated derivatives of the C^8O–OC^8 bridged dimers **13** and **14**, respectively (Scheme 2). The mass calculations imply that the silylated derivative of compound **13** (calcd 952.397 for $C_{36}H_{72}N_{10}O_7Si_7$) possesses only one deoxyribose sugar moiety, whereas that of **14** (calcd 764.31 for $C_{28}H_{56}N_{10}O_4Si_6$) has no sugar unit. It is believed that the deoxyribose sugar moiety of dGMP undergoes hydrolysis readily, due to the steric hindrance of the sugar units during dimerization. It was also noticed that if a deoxyribose sugar unit is preserved in the dimer, then, upon silylation, both reactive OH groups from the five-membered deoxyribose ring are rapidly silylated. In contrast, both in dimers and trimers, the NH_2 group from the guanine base, upon silylation, changes to $NHSi(CH_3)_3$ rather than $N[Si(CH_3)_3]_2$. Such observations

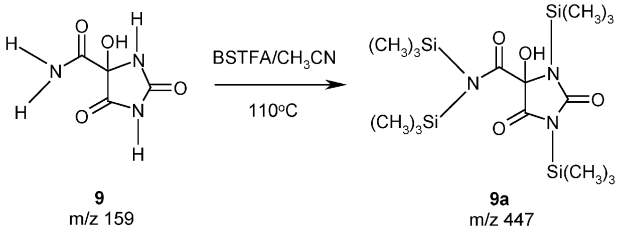

Scheme 1 Formation of the tetrasilylated derivative of 5-hydroxyhydantion-5-carboxamide by reaction with BSTFA in acetonitrile at pH 7.1.

View Article Online

Downloaded by University of California - Los Angeles on 01 January 2013
Published on 02 March 2005 on http://pubs.rsc.org | doi:10.1039/B415452P

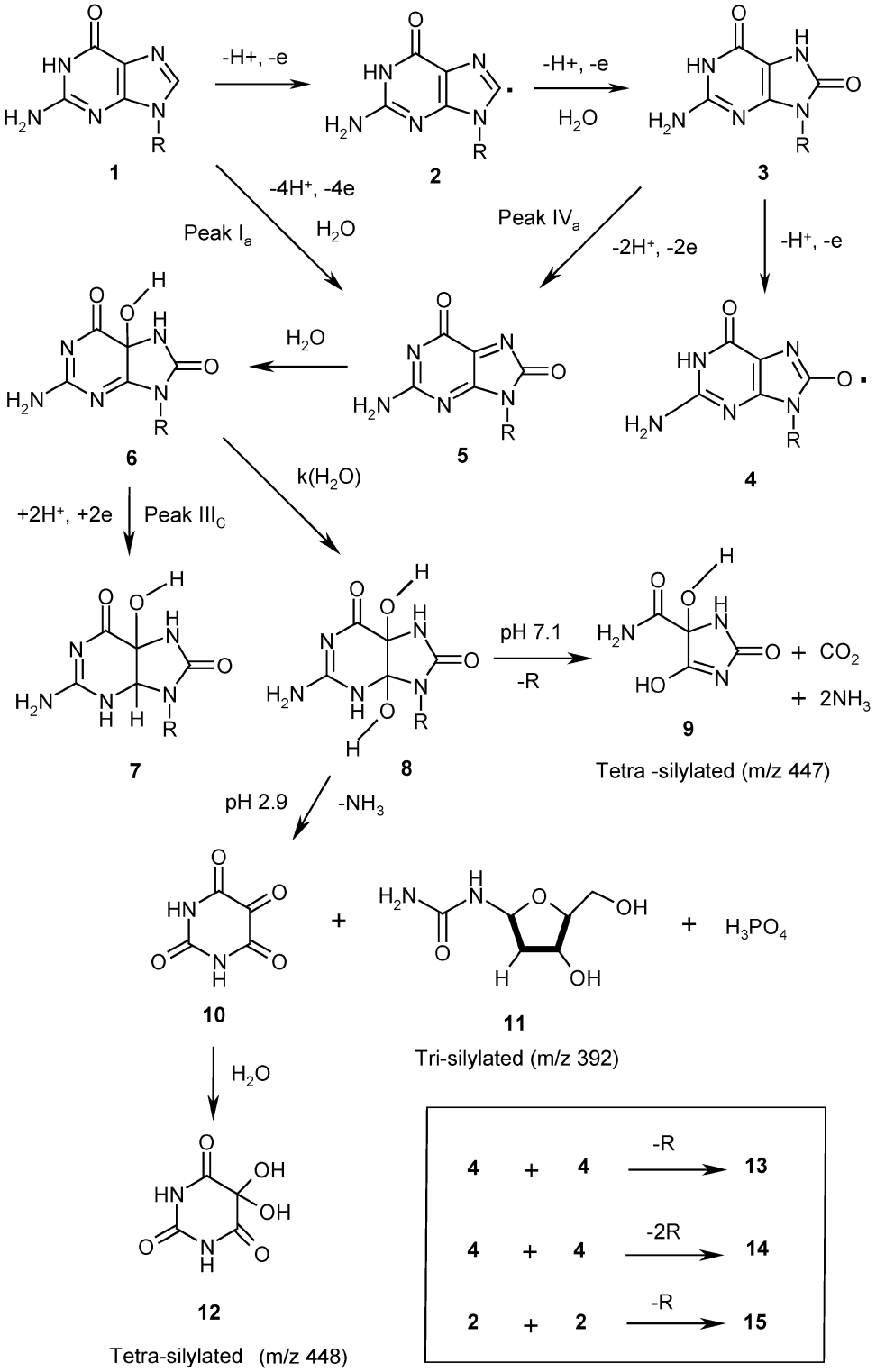

Scheme 2 Tentative redox mechanism explaining the formation of compounds **11–15**, depending on the pH and redox potential.

about the silylated molecules are also well-documented in the literature.[25,39] The fifth peak at R_t 9.88 min with m/z 920 (M^+; 15.6%), corresponds to the heptasilylated derivative of dimer **15** (calcd 920.407 for $C_{36}H_{72}N_{10}O_5Si_7$), having a C^8–C^8 linkage (Scheme 2). Formation of O–O and C–C-linked dimers during the oxidation of purine nucleosides and nucleotides is also reported in the literature.[26,39,40]

Attempts to separate the products for further characterization by standard analytical techniques were unsuccessful, due to the very similar retention times in HPLC. Despite our efforts, we found that separation of the dimers was impossible to achieve. However, when the bulk electrolysis of dGMP was carried out at pH 7.1 below $E_p(II_a)$, compound **9** could be isolated as a single oxidation product (TLC $R_f \sim 0.31$) and characterized by FTIR and ^{1}H NMR spectroscopy. **9** exhibited bands in the IR at $\nu_{max} = 661, 814, 1281, 1338, 1683$ (CONH), 1720, 1765 (C=O), 3220 and 3401 (NH) cm^{-1}. The ^{1}H NMR spectrum of compound **9** showed signals at $\delta = 10.71$ (br s, 1 H, O=C–NH–C=O), 7.95 (s, 1H, NH), and 6.62 (s, 2H, NH_2). However, no clear peak was observed for the tertiary hydroxyl proton. It is assumed that the missing peak is hidden under the water peak in DMSO-d_6. Upon D_2O exchange, all signals disappeared, except for a peak at 4.68 ppm from HDO. **9** presented all the characteristic features of 4-hydroxy-2,5-dioxoimidazolidine-4-carboxamide, thus confirming the MS assignment.

View Article Online

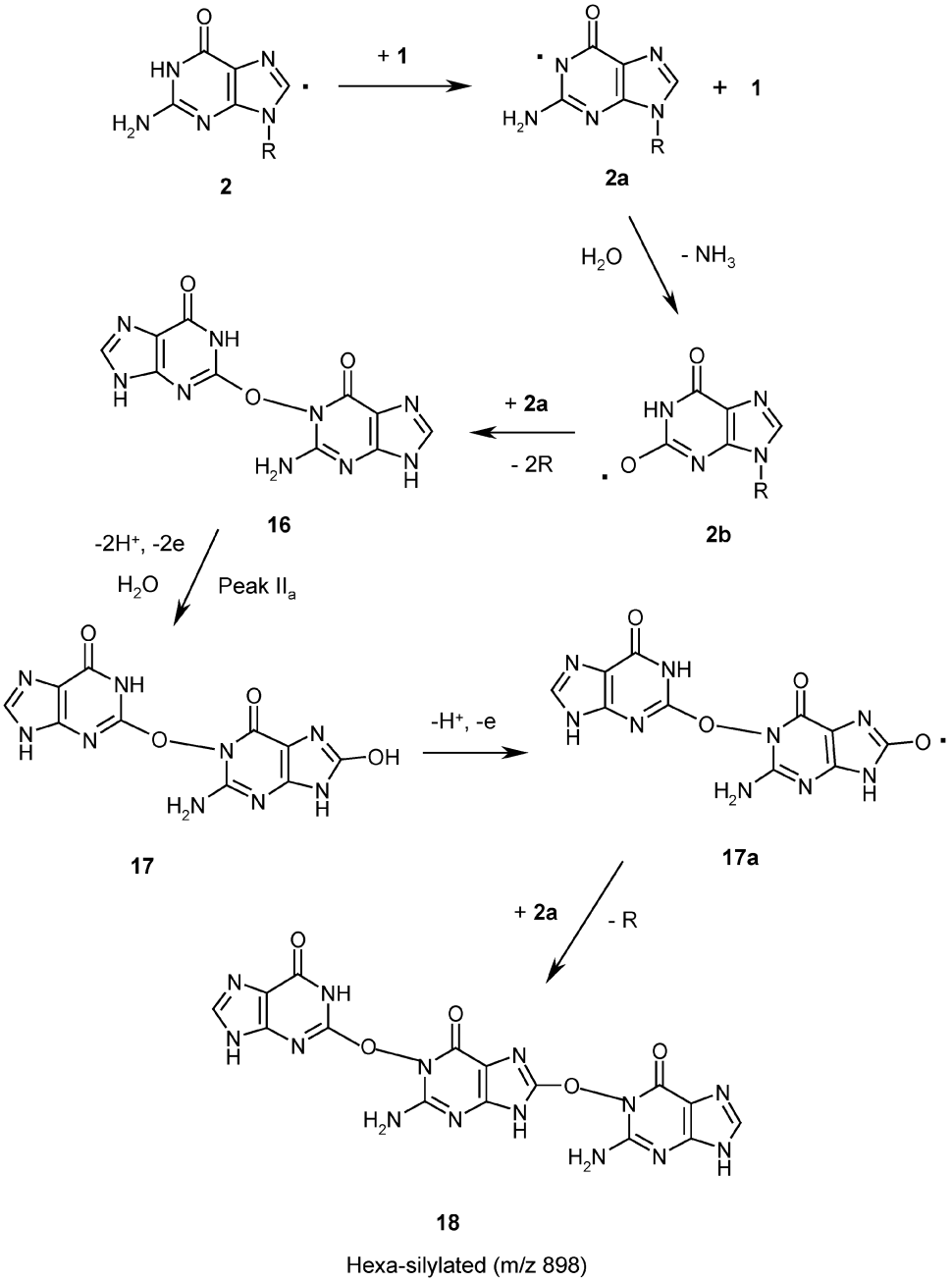

Scheme 3 Proposed mechanistic pathway for the formation of the N–O–C bridged trimer of dGMP at PGE.

Downloaded by University of California - Los Angeles on 01 January 2013
Published on 02 March 2005 on http://pubs.rsc.org | doi:10.1039/B415452P

Redox mechanism

Tentative redox mechanisms assigning the observed anodic and cathodic signals I–V to their corresponding reactions with the probable structure of the products formed during the electrooxidation of dGMP at pH 7.1 and 2.9 are given in Schemes 2 and 3. Experimental results revealed that the electrooxidation of dGMP occurs in an overall $4H^+$,$4e^-$ process, corresponding to peak I_a in CV. The $4H^+$,$4e^-$ process may occur in a single step or as the combination of two $2H^+$,$2e^-$ processes. The appearance of peak IV_a in the second positive sweep in CV suggests that oxidation occurs in two $2H^+$,$2e^-$ processes. In Scheme 2, peak IV_a is assigned to the oxidation of the 8-hydroxy dGMP, which can be more easily oxidized than dGMP. As the coulometric experiments suggest involvement of coupled chemical reactions, it seems reasonable

Table 3 MS data recorded at each retention time where peaks were detected from the silylated electrolyzed samples of dGMP at pH 7.1 and 2.9

pH	R_t/min	Product	M^+ ion peak	Fragmentation pattern
7.1	5.98	**9**	447	287 (11.4%); 259 (100%); 188 (15.1%); 160 (9.2%).
	6.42	**18**	898	618 (72.1%); 602 (13.4%); 604 (12.8%); 588 (8.3%); 309 (10.5%); 295 (25.1%); 293 (5.5%).
2.9	4.35	**11**	392	376 (10.7%); 348 (5.6%); 261 (100%); 131 (7.5%).
	7.35	**13**	952	691 (72.2%); 586 (5.5%); 570 (9.4%); 382 (7.8%); 293 (28.1%); 261 (15%).
	7.42	**14**	764	598 (10.6%); 382 (100%); 366 (16.8%); 253 (8.2%); 129 (9.5%).
	9.88	**15**	920	863 (5.0%); 659 (15.5%); 554 (85.4%); 366 (9.1%); 261 (50.5%).
	11.1	**12**	448	331 (13.5%); 270 (11.4%); 246 (100%); 115 (10.3%).

View Article Online

to conclude that the product of the primary electrode reaction is unstable and undergoes follow-up chemical reactions.

The first $1H^+,1e^-$ oxidation of dGMP (**1**) gives rise to a free radical **2** at the electrode surface, which is rapidly oxidized in the presence of water by a further $1H^+,1e^-$ process, yielding compound **3** (Scheme 2). The initial oxidation of purines at the C^8 position, generating a free radical, is well-documented in the literature.[41,42] The 8-hydroxy dGMP (**3**) can undergo oxidation by two different routes. In the first case a $1H^+,1e^-$ oxidation would lead to the formation of radical **4**, whereas in the second case a $2H^+,2e^-$ oxidation will give diimine **5**. It is expected that the potentials of both oxidation processes would be very close and, therefore, would explain that no separate peaks for such oxidations were observed by CV. The diimine (**5**) is expected to be highly unstable as previously reported for several purines[43,44] and, hence, it will be readily attacked by a water molecule to give the imine alcohol **6**. Conversion of **5** to **6** is a simple chemical reaction. The imine alcohol can be reduced at PGE in a $2H^+,2e^-$ process will give compound **7**. This reduction process is assigned to peak III_c. On the other hand, compound **6** can be further attacked by another molecule of water to give a diol **8**. The values of k observed for the kinetics of decay are correlated to the conversion of **6** to **8**, which appears to be a slow process ($k = \sim 5.05 \times 10^{-4}\ s^{-1}$). As the values of k observed were more or less similar at pH 2.9 and 7.1, it is reasonable to conclude that the rate of decay, that is, the reaction between **6** and a molecule of water, is independent of pH. At pH 7.1, the diol **8** undergoes opening of the pyrimidine ring to give 4-hydroxy-2,5-dioxoimidazolidine-4-carboxamide (5-hydroxyhydantoin-5-carboxamide, **9**) as one of the major electrooxidation products. It is interesting to note that compound **9** does not possess a ribosyl group. The riboside moiety of diol **8** seems to be hydrolyzed in aqueous solutions. At neutral pH, the rupture of the ribosyl bond during the pyrimidine ring-opening of purines is described in the literature.[45,46]

The formation of the second major product, trimer **18**, at pH 7.1 is mechanistically represented in Scheme 3 and its formation can also be explained by an EC mechanism as follows. The $1H^+,1e^-$ oxidation of **1** generates free radical **2** at the PGE surface. Radical **2** reacts with another molecule of **1** diffusing to the surface, forming the secondary radical **2a**, which corresponds to a hydrogen atom abstraction reaction. **2a** reacts with a water molecule to give another secondary free radical species **2b**, which rapidly combines with a second molecule of **2a** to lead to the formation of a reactive dimer **16**, in which both deoxyribose sugar units of the purine bases have been lost by hydrolysis. A $2H^+,2e^-$ oxidation of **16**, followed by attack by a water molecule, is expected to produce **17**. Dimer **17**, upon further $1H^+$ $1e^-$ oxidation gives rise to compound **17a** having a free radical at the oxygen atom attached to C_8. The free radical species **17a**, upon combination with another molecule of **2a**, yields **18** having a N–O–C^8 guanine base linkage. The molar mass of 898 corresponds to the hexasilylated derivative of compound **18**. The appearance of peak II_a in the cyclic voltammogram of dGMP at pH 7.1 could be due to the overall $3H^+,3e^-$ oxidation of dimer **16** into **18** as shown in Scheme 3. The biodegradation of dGMP is reported[47] to produce xanthine as one of its metabolites, which was not identified among the final products in the present study. Still, the radical **2b**, proposed here as an intermediate to **18** (Scheme 3), is a reactive moiety of the xanthine nucleotide. The identification of dimers and trimer formed during oxidation of dGMP strongly indicates that the radical–radical coupling reactions play a significant role in comparison to other reactions which lead to alloxan and urearibosides as the products.

Under acidic conditions (pH 2.9), the diol **8** exhibits a different behavior, the imidazole ring of the diol rupturing, with the loss of ammonia and H_3PO_4, to give alloxan **10** and urea deoxyriboside **11** (Scheme 2). As alloxan is readily hydrated at pH 2.9, a hydrated alloxan (**12**), namely 5,5-dihydroxypyrimidine-2,4,6-trione, is the actual product of the reaction, which was identified as its tetrasilylated derivative by GC-MS. The opening of the imidazole ring and the formation of alloxan in acidic conditions has been reported[27,48] for purines. Formation of the dimers (**13**, **14** and **15**) at pH 2.9 is possible by different combinations of the free radicals **2** and **4**, as shown in Scheme 2. The free radical **4** generated from **3** can rapidly dimerize to form the C^8O–OC^8 bridged dimers **13** and **14**, depending on whether one or two deoxyribose units are lost during the O–O bond formation at the C^8 position. Dimer **15** could result from the combination of two molecules of radical **2** through the C–C bond at the C^8 position. However, it must be realized that the proposed mechanistic pathway could be one out of several mechanisms by which the products can be formed. The most probable structures assigned for the dimers **13**, **14** and **15** are shown here.

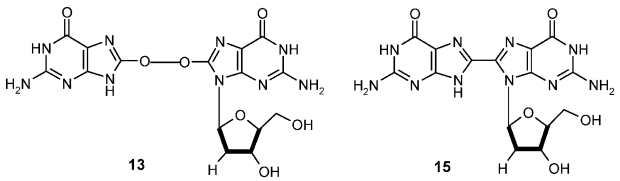

13
Hepta-silylated (m/z 952)

15
Hepta-silylated (m/z 920)

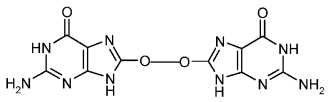

14
Hexa-silylated (m/z 764)

Conclusions

The present study clearly demonstrates that the electron-transfer reactions and redox mechanism of dGMP follow a complex pathway. By extension, this study provides invaluable information on the metabolic route of dGMP in the biosystem. It is likely that reactions, similar those involved in the electrooxidation of dGMP under oxidative conditions, may occur and yield tumorogenic products in the human organism. Our previous results on the electrochemical oxidation of guanosine[41] already reported that a dimer with an O–O linkage very similar to dimer **14** causes nephritis with oedema in albino mice and is toxic in nature. Identification of the different oxidation products of dGMP at PGE can provide a very important tool for the biochemist to understand oxidative damage in DNA. Although complex biological reactions of dGMP occur at the enzyme–solution interface, the study of its electrochemical behavior at the electrode–solution interface close to physiological conditions can be a perfect model system for *in vitro* studies.

Acknowledgements

One of the authors (AML) is thankful to the Indian Institute of Technology Roorkee (IITR) for awarding him an Institute Fellowship, sponsored by the Ministry of Human Resources Department (MHRD), Govt. of India. Financial assistance for this work was also provided by MHRD through IITR grant code no. 106-20-77.

References

1 G. Hardin and C. Bajema, *Biology: Its Principles and Implications*, W. H. Freeman and Co., San Francisco, 3rd edn., 1977, p. 102.
2 J. Taanman, J. R. Muddle and A. C. Mauntau, *Hum. Mol. Genet.*, 2003, **12**, 1839.

Downloaded by University of California - Los Angeles on 01 January 2013
Published on 02 March 2005 on http://pubs.rsc.org | doi:10.1039/B415452P

View Article Online

3 S. Eriksson, B. Munch-Petersen, K. Johansson and H. Eklund, *Cell Mol. Life Sci.*, 2002, **59**, 1327.
4 M. Taktakishvili and V. Nair, *Tetrahedron Lett.*, 2000, **41**, 7173.
5 T. S. Stolworthy, E. Krabbenhoft and M. E. Black, *Anal. Biochem.*, 2003, **322**, 40.
6 S. Pal and V. Nair, *Biotechnol. Lett.*, 1998, **20**, 1149.
7 H. Elisabeth and J. Roland, *Nutr. Res. (N.Y.)*, 2004, **24**, 197.
8 L. Z. Luo, K. M. Werner, S. M. Gollin and W. S. Saunders, *Mutat. Res.*, 2004, **554**, 375.
9 C. Lu, W. Lin, Z. Han, S. Yao and N. Lin, *Phys. Chem. Chem. Phys.*, 2000, **2**, 329.
10 C. Lu, S. Yao and N. Lin, *Chem. Phys. Lett.*, 2000, **330**, 389.
11 V. Shafirovich, J. Cadet, D. Gasparutto, A. Dourandin and N. E. Geacintov, *Chem. Res. Toxicol.*, 2001, **14**, 233.
12 Y. Shi, C. Huang, W. Wang, J. Kang, S. Yao, N. Lin and R. Zheng, *Radiat. Phys. Chem.*, 2000, **58**, 253.
13 Y. Jiang, W. Lin, S. Yao, N. Lin and D. Zhu, *Radiat. Phys. Chem.*, 1999, **54**, 349.
14 J. Ma, S. Qian, W. Lin and S. Yao, *Sci. China, Ser. B*, 1998, **41**, 556.
15 H. A. Tajmir-Riahi and T. Theophanides, *Inorg. Chim. Acta*, 1983, **30**, 223.
16 H. A. Tajmir-Riahi, *Biopolymers*, 1991, **31**, 1065.
17 J. Pan and F. Chung, *Res. Toxicol.*, 2002, **15**, 367.
18 S. Choi, R. B. Cooley, A. S. Hakemian, Y. C. Larrabee, R. C. Bunt, S. D. Maupas, J. G. Muller and C. J. Burrows, *J. Am. Chem. Soc.*, 2004, **126**, 591.
19 V. Duarte, J. G. Muller and C. J. Burrows, *Nucleic Acids Res.*, 1999, **27**, 496.
20 L. Torun and H. Morrison, *Photochem. Photobiol.*, 2003, **77**, 370.
21 A. M. Oliveira-Brett, J. A. P. Piedade, L. A. Silva and V. C. Diculescu, *Anal. Biochem.*, 2004, **332**, 321.
22 C. Prado, G. Flechsig, P. Gruendler, J. Foord, S. John, F. Marken and R. G. Compton, *Analyst (Cambridge, U.K.)*, 2002, **127**, 329.
23 G. Dryhurst, *Chem. Rev.*, 1990, **90**, 795.
24 T. Tabatabaie, R. N. Goyal, C. L. Blank and G. Dryhurst, *J. Med. Chem.*, 1993, **36**, 229.
25 R. N. Goyal, A. K. Jain and N. Jain, *J. Chem. Soc., Perkin Trans. 2*, 1996, 1153.
26 R. N. Goyal, P. Thankachan and N. Jain, *Bull. Chem. Soc. Jpn.*, 2000, **73**, 1515.
27 R. N. Goyal, A. Rastogi and A. Sangal, *New J. Chem.*, 2001, **25**, 545.
28 R. N. Goyal and A. Sangal, *J. Electroanal. Chem.*, 2003, **557**, 147.
29 G. D. Christian and W. C. Purdy, *J. Electroanal. Chem.*, 1962, **3**, 363.
30 J. L. Owens, H. A. Marsh and G. Dryhurst, *J. Electroanal. Chem.*, 1978, **91**, 231.
31 J. J. Lingane, *Electroanalytical Chemistry*, Wiley, New York, 2nd edn, 1966, p. 222.
32 R. S. Nicholson and I. Shain, *Anal. Chem.*, 1964, **36**, 706.
33 E. C. Brown and R. F. Large, in *Physical Methods of Chemistry*, eds. A. Weissberger and B. W. Rossiter, Wiley, New York, 1974, vol. **1**, p. 423.
34 G. Cauquis and V. D. Parker, in *Organic Electrochemistry*, ed. M. M. Baizer, Marcel Dekker, New York, 1973, p. 134.
35 A. A. Rostami and G. Dryhurst, *J. Electroanal. Chem.*, 1987, **223**, 143.
36 R. N. Goyal, *Indian J. Chem., Sect. A: Inorg., Bio-inorg., Phys., Theor. Anal. Chem.*, 1989, **28**, 467.
37 R. N. Goyal, A. K. Srivastava and V. Bansal, *J. Chem. Soc., Perkin Trans. 2*, 1994, 1709.
38 P. Subramanian and G. Dryhurst, *J. Electroanal. Chem.*, 1987, **224**, 137.
39 R. N. Goyal, A. Brajter-Toth, J. S. Besca and G. Dryhurst, *J. Electroanal. Chem.*, 1983, **144**, 163.
40 E. F. Strittmatter, P. D. Schnier, J. S. Klassen and E. R. Williams, *J. Am. Soc. Mass Spectrom.*, 1999, **10**, 1095.
41 R. N. Goyal, N. Jain and D. K. Garg, *Bioelectrochem. Bioenerg.*, 1997, **43**, 105.
42 L. P. Candeias and S. Steenken, *J. Phys. Chem.*, 1992, **96**, 937.
43 R. N. Goyal and G. Dryhurst, *J. Electroanal. Chem.*, 1982, **135**, 75.
44 G. Dryhurst, K. M. Kadish, F. Scheller and R. Renneberg, *Biological Electrochemistry*, Academic Press, New York, 1982, vol. **1**, p. 279.
45 T. E. C. Peterson and A. Brajter-Toth, *J. Electroanal. Chem.*, 1988, **239**, 161.
46 S. Y. Wang, *Photochemistry and Photobiology of Nucleic Acids*, Academic Press, New York, 1976, vol. **1**, p. 362.
47 H. Kruszewska, A. Misicka and U. Chmielowiec, *Il Farmaco*, 2004, **59**, 13.
48 J. L. Owens, H. H. Thomas and G. Dryhurst, *Anal. Chim. Acta*, 1978, **96**, 89.

Published on 02 March 2005 on http://pubs.rsc.org | doi:10.1039/B415452P
Downloaded by University of California - Los Angeles on 01 January 2013